JOURNAL OF SPACECRAFT AND ROCKETS
Vol. 48, No. 3, May–June 2011

Engineering Notes

Parameter Study on Pogo Stability of Liquid Rockets

Zhihua Zhao* and Gexue Ren†
Tsinghua University,
100084 Beijing, People's Republic of China
and
Ziwen Yu,‡ Bo Tang,‡ and Qingsong Zhang‡
China Academy of Launch Vehicle Technology,
100084 Beijing, People's Republic of China

DOI: 10.2514/1.51877

Nomenclature

A_s = cross-sectional area of suction line, m^2
A_{th} = nozzle throat area, m^2
C_f = thrust coefficient, dimensionless
g = standard gravitational acceleration, m/s^2
h_s = height of propellant in suction line, m
h_t = height of propellant in tank, m
I_s = inertance of propellant in suction line, s^2/m^2
K^* = effective stiffness of accumulator which is defined as $K_a K_p/(K_a + K_p)$, $1/m^2$
K_a = stiffness of the accumulator, $1/m^2$
K_p = stiffness of pump cavitation, $1/m^2$
k = the ratio between effective stiffness and stiffness of accumulator defined as K^*/K_a, dimensionless
L = length, m
M_s = modal mass of structure mode, kg
i, j, n = index, dimensionless
$m + 1$ = pump gain, dimensionless
N = number of thrust chambers, dimensionless
p = oscillatory pressure, Pa
R_c = linearalized combustion resistance for propulsion flow perturbation, s/m^2
w = weight displacement of flow, N
α = mass flow gain factor of a pump, s
β = the propulsion modal damping coefficient, dimensionless
γ = dimensionless mass flow gain factor of a pump defined as $\Omega\alpha$, dimensionless
κ = couple strength between the structure mode and the propulsion system, dimensionless
λ = frequency ratio between the propulsion mode and the structure mode, dimensionless
ξ = the structure damping ratio, dimensionless
ρ = density of the propellant, kg/m^3
φ = structural mode gain, dimensionless
Ω = circular natural frequency of the structure mode, $1/s$
ω = circular natural frequency of the propulsion mode, $1/s$

Subscripts

c = combustion chamber
p = pump
s = suction line
t = tank

Received 3 August 2010; revision received 25 December 2010; accepted for publication 9 January 2011.

*Ph.D. Candidate, School of Aerospace; aslan.zhao@tsinghua.org.cn.
†Professor, School of Aerospace; rengx@tsinghua.edu.cn.
‡Engineer, Department of System Design.

I. Introduction

POGO vibration has been suffered by most of powerful liquid rocket vehicles, such as the Titan 2 [1], the Diamond B [2], and the Saturn 5 [3]. Its potential threats on payload and pilot safety attracted researchers' attention since it is first encountered on Titan 2 in 1960s [4], and promoted extensive studies to understand and mitigate it especially from the massive Saturn 5 for the manned Apollo program [3,5–8].

Now, it has been well revealed by the linear model [4,9–13] that pogo phenomenon is a self-excited vibration due to instability arising from closed-loop interaction of the vehicle structure with the propulsion system, as shown in Fig. 1. And this instability tends to occur when the frequency of the propulsion system is close to that of the longitudinal structure modes [4,9,10]. Therefore, a natural way of avoiding pogo vibration is to separate the two frequencies and this idea has been successfully implemented by equipping the invented accumulator on Saturn 5 and the space shuttle [3,5,14,15].

Nevertheless, apart from frequencies of the propulsion and structure system, there are more than 10 other physical parameters affect the pogo stability margin and result the mission-specific performance. This might explain why a vehicle without pogo in one mission can be fully troubled in another with slightly different or even same payload [12,16]. To design a rocket which is pogo-free and robust in the sense that some uncertain payloads and variable working conditions will not destabilize it, it is necessary to understand the role of parameters on pogo stability. However, quantitative results are rarely found in available literature.

In this Note, we analytically investigate the role of physical factors on pogo stability and the parameter domain of robust stability. For simplicity, a simple coupling system between a longitudinal structure mode and a reduced single-propellant system is addressed to offer a preliminary and overall view. The propulsion system is shown in Fig. 2, it includes six components, i.e., tank, suction line, junction, accumulator, pump, and thrust chamber. And the main assumptions are the following:

1) The propellant is considered as incompressible.
2) The resistance of suction line is omitted.
3) The duct between accumulator and pump, and the discharge duct segment between pump and thrust is neglected.
4) The inertial and resistance of accumulator and pump is neglected.

The modeling work for such propulsion system is greatly simplified while the essential mechanisms of pogo instability are reserved. Under those assumptions, the governing equations of the closed loop are derived. Then, it is shown that system stability is completely governed by five dimensionless parameters expressed by the combination of all physical factors. Furthermore, the governing equation of boundary surface between stable and unstable is explicitly formulated. Based on it, the sensitive and robust parameter domain for pogo stability is extensively studied.

II. Simplified Single-Propellant Model

Here, we adopt the same governing equations as [10] or [17] to model structure and propulsion system. Hereafter, all pressures and weight flows are oscillatory perturbations.

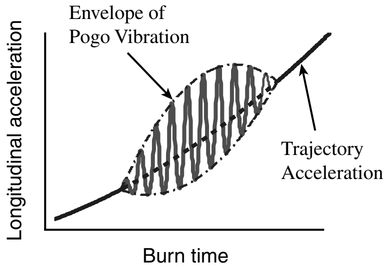

a)

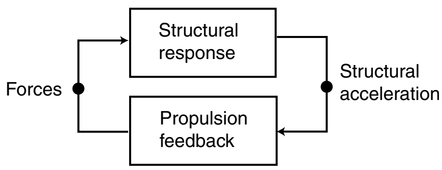

b)

Fig. 1 Typical pogo vibration and block diagram of closed loop in pogo: a) typical pogo vibration and b) block diagram of closed loop in pogo.

A. Structure Mode

The governing equation for a structure mode is

$$\ddot{q} + 2\xi\Omega\dot{q} + \Omega^2 q = -\frac{A_{\text{th}} C_f N \varphi_c}{M_s} p_c \tag{1}$$

where q, Ω, ξ and M_s are the generalized coordinate, circular nature frequency, structure damping ratio and generalized mass of structure mode, φ_c is the structural mode gain at the thrust, N is the number of thrusts connected by the suction line, A_{th}, C_f and p_c are the nozzle throat area, thrust coefficient and the chamber pressure, respectively, which feature the feedback from propellant system to the structure.

B. Propellant in Tank

The pressure at the bottom of the tank or the top of the suction line is

$$p_t = -\rho h_t \varphi_t \ddot{q} \tag{2}$$

where ρ is the density of propellant, h_t is the height of propellant in tank, φ_t is the structural mode gain at the mass center of the tank, and the top dot stands for the derivative with respect to time t.

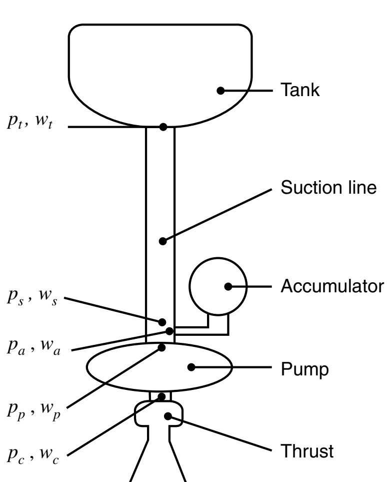

Fig. 2 Typical components of a single-propellant system.

C. Suction Line

The propellant in suction line is considered as incompressible. Then it satisfies

$$p_t - p_s = I_s \ddot{w}_s + \rho h_s \varphi_s \ddot{q} \tag{3}$$

where p_s and w_s are the pressure and the weight displacement of the fluid at the output of the suction line, respectively, I_s and h_s are the inertia and vertical height of propellant in suction line, respectively, and φ_s is structural mode gain at the bottom of the suction line.

D. Junction

The junction joints three elements together: the suction line, accumulator, and pump. So,

$$\begin{cases} p_s = p_p = p_a \\ w_s = w_a + w_p \end{cases} \tag{4}$$

where p_p, w_p are the pressure and weight displacement of flow at the input of pump, and p_a, w_a are the pressure and weight displacement of flow at the input of accumulator.

E. Accumulator

The inertance and resistance of accumulator is neglected, thus accumulator works like a soft spring, or in other words

$$p_a = K_a w_a \tag{5}$$

where K_a is the tangent stiffness of accumulator from its state of equation.

F. Pump

Neglecting the pump inertance and resistance, then the governing equation for pump becomes

$$\begin{cases} p_c = (m+1) p_p \\ p_p = K_p (w_p - w_{\text{c}}) - \alpha \dot{w}_p \end{cases} \tag{6}$$

where p_c, w_c are the pressure and weight displacement of flow at the output of pump, K_p, $m+1$, and α are the stiffness of pump cavitation, pressure gain and mass flow gain factor of the pump.

G. Thrust Chamber

Single propellant is focused in this Note, and the combustion time lag of thrust is ignored since the experimental values are usually small and its effects on pogo instability can be neglected. Thus, we have

$$p_c = R_c \dot{w}_c \tag{7}$$

where R_c is often called combustion resistance of thrust.

After combing and simplifying Eqs. (1–7), the coupled system is described by three equations as

$$\begin{gathered} q'' + 2\xi\Omega q' + \Omega^2 q = -\frac{(m+1) A_{\text{th}} C_f N \varphi_c}{M_s} R_c^* w_c' \\ w_s'' + \frac{R_c^*}{I_s} w_c' = -\rho \frac{h_t \varphi_t + h_s \varphi_s}{I_s} q'' \\ (w_s - w_c) - \alpha\left(w_s' - \frac{R_c^*}{K_a} w_c'' \right) = \frac{1}{K^*} w_c' \end{gathered} \tag{8}$$

where $R_c^* \equiv R_c/(m+1)$, and

$$K^* \equiv \frac{K_a K_p}{K_a + K_p} \tag{9}$$

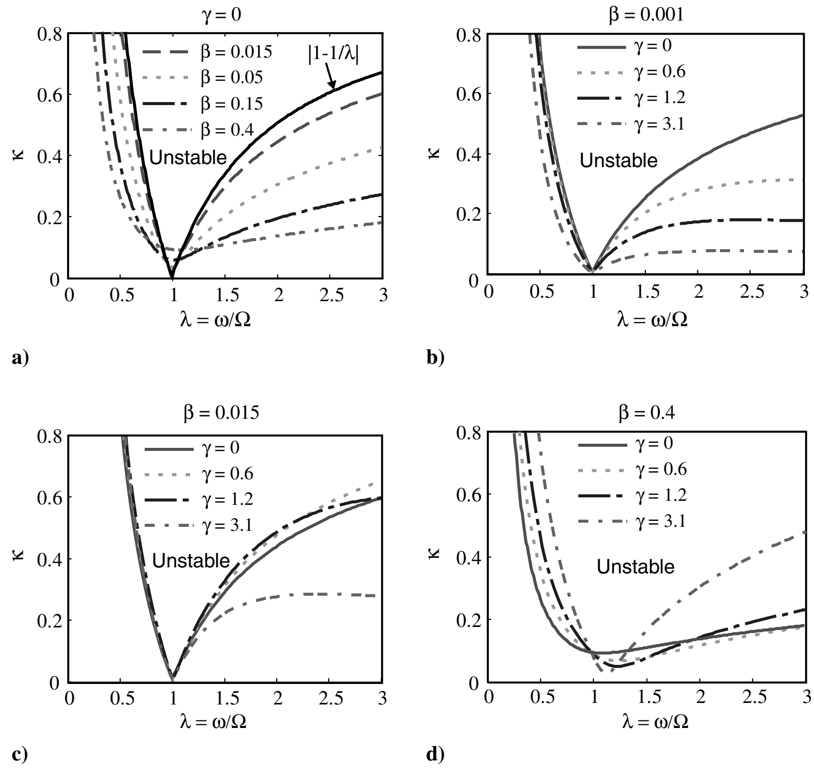

Fig. 3 Boundary curves between stable and unstable for different β and γ in κ-λ plane, with $\xi = 0.005$ and $k = 1$.

is defined as the effective stiffness of accumulator, which is smaller than K_a because the gas in accumulator and the bubble in pump are parallel working together. In case of pump mass flow gain is zero, the coupled system is simplified into two coupled oscillators:

$$\begin{cases} \ddot{q} + 2\xi\Omega\dot{q} + \Omega^2 q = -\chi v \\ \ddot{v} + 2\beta\omega\dot{v} + \omega^2 v = -\eta\omega^2\ddot{q} \end{cases} \tag{10}$$

where $\omega = \sqrt{K^*/I_s}$ is the circular natural frequency of the propulsion mode, $v = K^*(w_1 - w_c)$ characterizes the vibration of propellant, $\beta = (m^* + 1)I_s\omega/2R_c$ is the damping ratio of the propulsion mode, and

$$\chi \equiv \frac{(m+1)NA_{\text{th}}C_f\varphi_c}{M_s}, \qquad \eta = \rho(h_s\varphi_s + h_t\varphi_t)$$

are two parameters describing the strength of interaction between the structure mode and the propulsion mode.

According to the linear stability theory, if all eigenvalues of Eq. (8) have negative real parts, then system is asymptotically stable; otherwise neutrally stable or unstable [18]. For convenience of the solution of the eigenvalue problem, we rewrite Eq. (8) into matrix form:

$$[M][\ddot{x}] + [C][\dot{x}] + [K][x] = 0 \tag{11}$$

where

$$[x] = \begin{bmatrix} q \\ w_s \\ w_c \end{bmatrix}, \qquad [M] = \begin{bmatrix} 1 & 0 & 0 \\ \frac{\eta}{I_s} & 1 & 0 \\ 0 & 0 & \alpha R_c^*/K_a \end{bmatrix}$$

$$[C] = \begin{bmatrix} 2\xi\Omega & 0 & \chi R_c^* \\ 0 & 0 & \frac{R_c^*}{I_s} \\ 0 & -\alpha & -1/K^* \end{bmatrix}, \qquad [K] = \begin{bmatrix} \Omega^2 & 0 & 0 \\ 0 & 0 & 0 \\ 0 & 1 & -1 \end{bmatrix} \tag{12}$$

Assume an eigensolution has the following form:

$$[x] = [y]e^{Z\Omega t} \tag{13}$$

then we have

$$((Z\Omega)^2[M] + Z\Omega[C] + [K])[y] = 0$$

Nontrivial solution means the determinant of the coefficient matrix in the preceding equation has to be zero, i.e., Z satisfies a polynomial equation:

$$a_5Z^5 + a_4Z^4 + a_3Z^3 + a_2Z^2 + a_1Z + a_0 = 0 \tag{14}$$

and the five coefficients are

$$\begin{aligned} &a_0 = \lambda^2, \qquad a_1 = 2\xi\lambda^2 + 2\lambda\beta - \lambda^2\gamma \\ &a_2 = \lambda^2 + 1 - \lambda^2\kappa^2 + 4\xi\lambda\beta - 2\xi\lambda^2\gamma \\ &a_3 = 2\lambda\beta + 2\xi - (k + \lambda^2 - \lambda^2\kappa^2)\gamma \\ &a_4 = 1 - 2\xi\gamma k, \qquad a_5 = -\gamma k \end{aligned} \tag{15}$$

where, $\gamma = \Omega\alpha$, $k = K^*/K_a$ is the ratio between effective stiffness and stiffness of accumulator, $\lambda = \omega/\Omega$ is the frequency ratio between the frequency of propulsion and structure, and

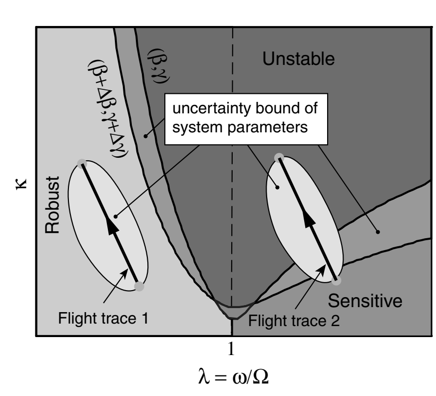

Fig. 4 Typical flight traces rockets leave in parameter space.

Table 1 The effects of physical parameters on the stability

Increasing parameters	λ	κ	α	γ	Effects on stability
$m+1$	—	↑	↑	—	Negative
α	—	—	—	↑	Ambiguous
$(h_t\varphi_t + h_s\varphi_s)\varphi_c/M_s$	—	↑	—	—	Negative
ω	↑	—	↑	—	Negative when λ < 1, positive when λ > 1
Ω	↓	—	—	—	Positive when λ < 1, negative when λ > 1
I_s	—	—	↑	—	Positive in most cases
R_c	—	—	↓	—	Positive in most cases
Order of structure mode	↓	↓	—	—	Positive

$$\kappa = \sqrt{\chi\eta} = \sqrt{\rho(h_t\varphi_t + h_s\varphi_s)(m+1)NA_{\text{th}}C_f\frac{\varphi_c}{M_s}} \tag{16}$$

is dimensionless variable named as couple strength of the structure mode and the propulsion system. Obviously, vehicle's pogo stability is completely governed by 5 dimensionless parameters, κ, λ, β, γ, and k in addition to structure damping ratio ξ. And by further algebraic manipulation, the boundary surface between stable and unstable region can be expressed through

$$(a_3a_0 - a_2a_1)(a_5a_2 - a_3a_4) - (a_0a_5 - a_1a_4)^2 = 0 \tag{17}$$

III. Results

To offer a straightforward understanding on boundary surface in the parameter space for the stability roots from Eq. (17), we project it into κ-λ plane by fixing two parameters ξ and k, while varying one parameter β or γ. As illustrated in Fig. 3, κ-λ plane is classified into two regions, unstable and stable one, by the boundary line. The region above the boundary line is unstable, and the remaining is stable. During analysis, typical value 0.005 is assigned for ξ, and 1 for k taking into account $K^* \approx K_a$ when accumulator is equipped into propulsion system.

Figure 3a shows that when $\gamma = 0$, the unstable region increased monotonously with the increase of propulsion modal damping β. While Figs. 3b–3d say γ may both expands and reduces the unstable region for different β. However, all of figures evident that both β and γ effect pogo stability greatly at λ > 1 interval, while little at λ < 1 interval.

It is worth to analysis the flight trace rocket leaves in κ-λ plane. During flight, κ grows rapidly, λ decreases quickly, γ changes slowly and β increases slowly, because the time dependent parameter Ω and $(h_t\varphi_t + h_s\varphi_s)\varphi_c/M_s$ grows rapidly while ω changes slowly. Therefore, as shown in Fig. 4, flight trace 1 and 2 are two typical traces rocket leaves in κ-λ plane. During flight, β locates at the range $(\beta, \beta + \Delta\beta)$, and γ locates at the range $(\gamma, \gamma + \Delta\gamma)$, then flight trace 2 starting from the domain of λ > 1 is easy to break the stability boundary while flight trace 1 starting from λ < 1 remains in the stable domain. The margin of flight trace 1 for stability is larger to counter the uncertainties system parameters. This result means λ < 1 is the parameter domain for robust vehicle. Thus, λ > 1 is referred as sensitive region while λ < 1 is robust region.

In addition, the roles of physical parameters on pogo stability are listed in Table 1 by checking its effects on varying trend of λ, κ, γ and β. Here, symbols ↑, — and ↓ represent increase, unchanged and decrease, respectively. For example, increasing $m+1$ is bad or negative for pogo stability since it enlarges both κ and β, while decreasing ω is good or positive since it decreases β and λ simultaneously. On the other hand, higher structure mode both have small κ and λ because of the increasing of the generalized mass M_s and circular natural frequency Ω, which are good for achieving stability. This means the pogo instability is hard to occur on high order structure mode, which is consistence with the historical observation.

IV. Conclusions

In this Note, an analytical result is obtained for the pogo stability problem of the heuristic system, i.e., a simplified single-propellant system coupled with a structure mode. It shows that the stability of the system is governed by a number of dimensionless parameters, including the frequency ratio λ, the couple strength κ, the propulsion modal damping β, the dimensionless mass flow gain factor γ and the ratio between effective stiffness and stiffness of accumulator k. The stability of the system is characterized in the parameter space with two domains, corresponding to λ < 1 and λ > 1 respectively. And the effects of physical parameters, such as pump gain and mass flow gain of pump, on pogo stability are clearly revealed. By checking the margin of parameter locus of a launching rocket in the stability domain, it is shown that pogo stability in the domain of λ < 1 is robust under parameter perturbation and launching parameter transition. Therefore, regulate the frequency of propulsion mode with accumulator until it is lower than that of the structure mode is a robust design to achieve pogo stability.

References

[1] Wagner, R. G., and Rubin, S., "Detection of Titan Pogo Characteristics by Analysis of Random Data," *Proceedings of ASME Symposium on Stochastic Processes in Dynamical Problems*, Los Angeles, 1969, pp. 51–62.

[2] Dordain, J. J., Lourme, D., and Estoueig, C., "Study on Pogo Effect on Launchers Europa-2 and Diamond-B," *Acta Astronautica*, Vol. 1, No. 11-1, 1974, pp. 1357–1384. doi:10.1016/0094-5765(74)90081-2

[3] Worlund, A. L., Hill, R. D., and Murphy, G. L., "Saturn 5 Longitudinal Oscillation (POGO) Solution," AIAA Paper 1969-548, 1969.

[4] Walker, J. H., Winje, R. A., and McKenna, K. J., "An Investigation of Low Frequency Longitudinal Vibration of the Titan 2 Missile During Stage 1 Flight," TRW Space Technology Labs Rept. 6438-6001-RU-000, March 1964.

[5] Castenholz, P. D., "Investigation of 17-Hz Closed-Loop Instability on S-2 Stage of Saturn 5," NASA CR-144131, Aug. 1969.

[6] Ryan, R. S., Kiefling, L. A., Buchanan, H. J., and Jarvinen, W. A., "Simulation of Saturn 5 S-2 Stage Propellant Feedline Dynamics," *Journal of Spacecraft and Rockets*, Vol. 7, No. 12, 1970, pp. 1407–1412. doi:10.2514/3.30182

[7] Ryan, R. S., Papadopoulos, J. G., Kiefling, L. A., Odum, R., Jarvinen, W., and Kennoy, J., "A Study of Saturn AS-502 Coupling Longitudinal Structural Vibration and Lateral Bending Response During Boost," *Journal of Spacecraft and Rockets*, Vol. 7, No. 2, 1970, pp. 113–118. doi:10.2514/3.29884

[8] Rubin, S., *Prevention of Coupled Structure-Propulsion Instability (POGO)*, AIAA Paper SP-8055, Oct. 1970.

[9] Radovcich, N. A., "Analytical Model for Missile Axial Oscillation Induced by Engine-Structure Coupling," Lockheed Missiles and Space Co. Rept. A658522, March 1965.

[10] Rubin, S., "Longitudinal Instability of Liquid Rockets due to Propulsion Feedback (POGO)," *Journal of Spacecraft and Rockets*, Vol. 3, No. 8, 1966, pp. 1188–1195. doi:10.2514/3.28626

[11] Iacopozzi, M., Lignarolo, V., and Prevel, D., "Pogo Characterisation of Ariane 5 Turbopump LOX Pump with Hot Water," AIAA/SAE/ASME/ASEE 29th Joint Propulsion Conference and Exhibit, AIAA Paper 1993-2124, Monterey, CA, 1993.

[12] Shimura, T., "The Effects of Geometry in the Dynamic Response of the Cavitating LE-7 LOX Pump," AIAA/SAE/ASME/ASEE 29th Joint Propulsion Conference and Exhibit, AIAA Paper 1993-2126, Monterey, CA, 1993.

[13] Dotson, K. W., Rubin, S., and Sako, B. H., "Effects of Unsteady Pump Cavitation on Propulsion–Structure Interaction (POGO) in Liquid

Rockets," 45th AIAA/ASME/ASCE/AHS/ASC Structures, Structural Dynamics and Material Conference, AIAA Paper 2004-2027, Palm Springs, CA, 2004.
[14] Rubin, S., Wagner, R. G., and Payne, J. G., "Pogo Suppression on Space Shuttle Early Studies," AIAA Paper CR-2210, March 1973.
[15] Larsen, C. E., "NASA Experience with Pogo in Human Spaceflight Vehicles," Johnson Space Center Rept. RTO-MP-AVT-152, May 2008.
[16] Dotson, K. W., Rubin, S., and Sako, B. H., "Mission-Specific Pogo Stability Analysis with Correlated Pump Parameters," *Journal of Propulsion and Power*, Vol. 21, No. 4, 2005, pp. 619–626. doi:10.2514/1.9440
[17] Oppenheim, B. W., and Rubin, S., "Advanced Pogo Stability Analysis for Liquid Rockets," *Journal of Spacecraft and Rockets*, Vol. 30, No. 3, 1993, pp. 360–373.
[18] Nayfeh, A. H., and Mook, D. T., *Nonlinear Oscillations*, Wiley, New York, 1979.

L. Peterson
Associate Editor